Bragg reflection of terahertz waves in plasmonic crystals

Eui Su Lee,[1] D.H. Kang,[2] A.I. Fernandez-Dominguez,[3] F.J. Garcia-Vidal,[3] L. Martin-Moreno,[4] D.S. Kim,[2] and Tae-In Jeon,[1]*

[1]Division of Electrical and Electronics Engineering, Korea Maritime University, Busan 606-791, Korea
[2]School of Physics and Astronomy, Seoul National University, Seoul 151-747, Korea
[3]Departamento de Fisica Teorica de la Materia Condensada, Universidad Autonoma de Madrid, E-28049, Spain
*[4]Instituto de Ciencia de Materiales de Aragón (ICMA) and Departamento de Física de la Materia Condensada,
CSIC-Universidad de Zaragoza, E-50009 Zaragoza, Spain*
*[*jeon@hhu.ac.kr](mailto:jeon@hhu.ac.kr)*

Abstract: We present experimental and theoretical studies on terahertz surface plasmon (TSP) propagation on slit and rectangular aperture arrays in an aluminum sheet. Terahertz waves are coupled onto the plasmonic structures via a parallel plate waveguide. Long-lasting oscillations are observed in the temporal pulse shape after propagating through the periodic structure, whose Fourier transformation into the frequency domain results in Bragg-resonance spectral features. We show that the interference between the incident wave and the radiation reflected from both the aperture array and the waveguide block is responsible for this Bragg-resonance behavior. The reflection coefficient for a single slit is deduced to be 0.017 ± 0.002.

References and links

1. A. Sommerfeld, "Ueber die fortpflanzung elektrodynamischer wellen längs eines drahtes," Ann. Phys. Chem. **303**(2), 233–290 (1899).
2. J. Zenneck, "Fortplfanzung ebener elektromagnetischer Wellen längs einer ebenen Leiterfläche," Ann. Phys. **23**, 846–866 (1907).
3. R. Mendis, and D. Grischkowsky, "Undistorted guided-wave propagation of subpicosecond terahertz pulses," Opt. Lett. **26**(11), 846–848 (2001).
4. K. Wang, and D. M. Mittleman, "Metal wires for terahertz wave guiding," Nature **432**(7015), 376–379 (2004).
5. R. H. Ritchie, "Plasma Losses by Fast Electrons in Thin Films," Phys. Rev. **106**(5), 874–881 (1957).
6. J. G. Rivas, and C. Schotsch, P. Haring Bolivar, and H. Kurz, "Enhanced transmission of THz radiation through subwavelength holes," Phys. Rev. B **68**(20), 201306 (2003).
7. J. G. Rivas, M. Kuttge, P. H. Bolivar, H. Kurz, and J. A. Sánchez-Gil, "Propagation of surface plasmon polaritons on semiconductor gratings," Phys. Rev. Lett. **93**(25), 256804 (2004).
8. J. B. Pendry, L. Martín-Moreno, and F. J. Garcia-Vidal, "Mimicking surface plasmons with structured surfaces," Science **305**(5685), 847–848 (2004).
9. F. J. Garcia-Vidal, L. Martin-Moreno, and J. B. Pendry, "Surfaces with holes in them: new plasmonic metamaterials," J. Opt. A, Pure Appl. Opt. **7**(2), S94 (2005).
10. C. R. Williams, S. R. Andrews, S. A. Maier, A. I. Fernandez-Dominguez, L. Martin-Moreno, and F. J. Garcia-Vidal, "Highly confined guiding of terahertz surface plasmon polaritons on structured metal surfaces," Nat. Photonics **2**(3), 175–179 (2008).
11. A. P. Hibbins, B. R. Evans, and J. R. Sambles, "Experimental verification of designer surface plasmons," Science **308**(5722), 670–672 (2005).
12. D. Qu, D. Grischkowsky, and W. Zhang, "Terahertz transmission properties of thin, subwavelength metallic hole arrays," Opt. Lett. **29**(8), 896–898 (2004).
13. J. A. Sánchez-Gil, and J. Gómez Rivas, "Thermal switching of the scattering coefficients of terahertz surface plasmon polaritons impinging on a finite array of subwavelength grooves on semiconductor surfaces," Phys. Rev. B **73**(20), 205410 (2006).
14. S. A. Maier, and S. R. Andrews, "Terahertz pulse propagation using plasmon-polariton-like surface modes on structured conductive surfaces," Appl. Phys. Lett. **88**(25), 251120 (2006).
15. J. T. Shen, P. B. Catrysse, and S. Fan, "Mechanism for designing metallic metamaterials with a high index of refraction," Phys. Rev. Lett. **94**(19), 197401 (2005).
16. T.-I. Jeon, and D. Grischkowsky, "THz Zenneck surface wave (THz surface plasmon) propagation on a metal sheet," Appl. Phys. Lett. **88**(6), 061113 (2006).

17. E. S. Lee, J. S. Jang, S. H. Kim, Y. B. Ji, and T.-I. Jeon, "Propagation of Single-Mode and Multi-Mode Terahertz Radiation Through a Parallel-Plate Waveguide," J. Korean Phys. Soc. **53**, 1891 (2008).
18. C. Ropers, D. J. Park, G. Stibenz, G. Steinmeyer, J. Kim, D. S. Kim, and C. Lienau, "Femtosecond light transmission and subradiant damping in plasmonic crystals," Phys. Rev. Lett. **94**(11), 113901 (2005).
19. F. López-Tejeira, F. J. García-Vidal, and L. Martín-Moreno, "Scattering of surface plasmons by one-dimensional periodic nanoindented surfaces," Phys. Rev. B **72**(16), 161405 (2005).
20. J. D. Jackson, "Classical Electrodynamics" (John Wiley & Sons, New York, 3rd edition, 1999).

1. Introduction

Zenneck and Sommerfeld in the beginning of the 20th century theoretically demonstrated that electromagnetic (EM) waves can propagate on a flat metal surface [1] and a cylindrical metal wire [2], respectively. Recently, subpicosecond THz pulses have been guided between two metal plates using a parallel-plate waveguide (PPWG) [3]. PPWG is good coupling tool to generate surface plasmon on metal surface. Zenneck and Sommerfeld in terahertz (THz) frequency were demonstrated on aluminum plate and single metal wire surface [4]. The electron plasma oscillations in a flat metal surface support surface plasmon polaritions (SPP's) [5]. However, the higher confinement of THz surface plasmons (TSPs) at flat interfaces requires a different method such as using highly doped semiconductors [6,7] because the fundamental plasma frequency of the metals falls in the ultraviolet part of the spectrum. Alternatively, a periodic array of apertures milled on a metal surface also supports geometrically induced or spoof SPPs [8,9]. Specifically, few hundred micron size patterns in a metal surface induce spoof SPPs in the THz frequency range [10]. In the effective medium picture, evanescent fields penetrate into the plasmonic structures akin to SPPs at visible frequencies. Geometrically induced SPPs were firstly verified in reflection experiments on substrates perforated with holes at Gigahertz frequencies [11]. Recently, THz transmission properties have been studied using thin and subwavelength metallic hole arrays [12]. Also, THz spoof surface plasmons have been studied theoretically in grooved [13] and dimpled structures [14]. Metal film with periodic slits can be considered an effective dielectric slab when the slit width is smaller than the wavelength of the propagation wave. The slits improve the bound-ness of surface waves on metal [15]. In this paper, we investigate, experimentally and theoretically, THz surface-bound waves propagating on periodic plasmonic structures such as slit and rectangular apertures. We experimentally deduce the reflection coefficient by single apertures, and compare with theory.

2. Experimental setup

The experimental apparatus is illustrated schematically in Fig. 1(a). A PPWG is used to couple the air traveling THz pulses to the Al sheet which is located between the two Al PPWG blocks. The coming out THz radiation is composed of a free space wave and bounded surface wave (Zenneck wave) on the Al sheet [16]. Most of the free space THz wave propagates close the Al surface, but slowly increasing –z-distance as it advances. The distance from the surface at the end of Al sheet to the center of the free space wave is about 3mm by FDTD simulation. Since the most of field intensity of the free space wave is radiated in the air, the free space wave effect was not explicitly considered in analysis. There is a 100μm wide air-gap between the surface of the Al sheet and the bottom surface of the upper waveguide block to generate a single mode THz wave. The plano-cylindrical lens produces a line focus on the input air gap. Since the incoming THz wave polarization (z-direction which is parallel to optical table) is perpendicular to the waveguide block's surface, only TM modes are generated. As the PPWG has a 100μm air-gap, the first two cutoff frequencies are 1.5 and 3 THz for odd and even modes respectively [17]. Because the integration of the odd field is zero, only even field can be detected. Since there is a little signal above 3THz in our spectrum, we conclude that only the TEM mode pulse propagates through the PPWG.
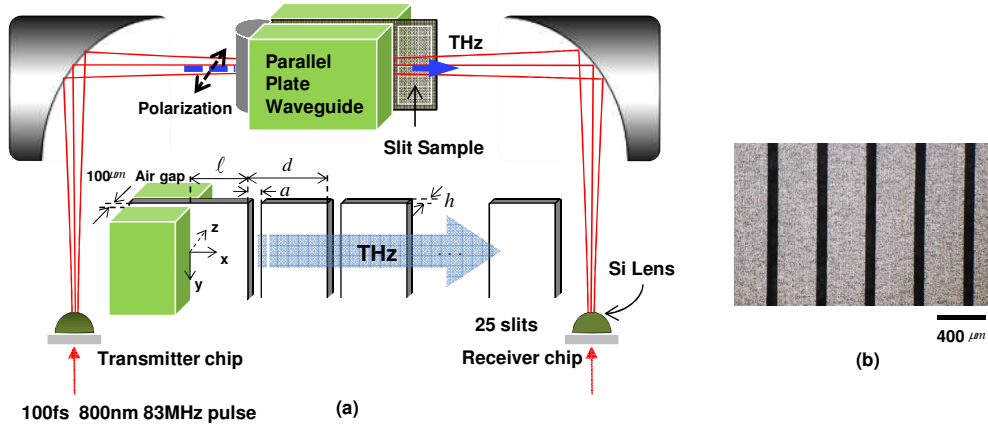
Fig. 1. (a) Experimental setup and geometry of the slit apertures. (b) Photo image of slits

The Al sheet extends outside of the waveguide block. The slits are made by micro photo chemical etching (Youngjin Astech Co.) and Fig. 1(b) shows the photo image of the slit edges. The slit array is located at $\ell = 480\mu m$ away from the edge of the waveguide block, with each slit having a 80μm width (*a*), 10mm length (that we consider as infinite), 50μm thickness (*h*), and 400μm slit-to-slit separation (*d*). The array is comprised by 25 slits perforated in the Al sheet. The generated TSPs propagate on the slit array and radiate into air at the end of Al sheet. Because of the easy coupling of TSP pulses into freely propagating radiation [16], these can be detected by the THz time-domain spectroscopy system as shown in Fig. 1(a).

3. Measurements and analysis

Measurements of the TSP signal radiated at the end of the Al sheet are shown in Fig. 2(a). The main THz pulse caused by the free space wave and TSP without slits effect. The well defined oscillation pulses caused by the slits appear after the main TSP pulse. We note that the quasi-period of the long-term oscillation is about 2.66ps, which corresponds to the round-trip time over the array period, suggesting Bragg-reflection effects. Indeed, Fig. 2(b) shows the Fourier-transform of later-time traces from 10ps to 55ps, displaying now prominent spectral peaks that is spaced by $0.375\text{THz} \approx \dfrac{c}{2d}$. The physics behind the appearance of these frequency components is as follows: when the main TSP pulse propagates through a slit, the majority of the TSP pulse keeps travelling along the forward direction while a small fraction is reflected by the slits. The reflected wave travels backward and is then strongly reflected by the waveguide block, again propagating forward. The interference between many of these events leads to the measured spectrum, shown in the inset of Fig. 2(b). Thus, the measured THz TSP spectrum can be expressed as

$$E(\omega) = E_{ref}(\omega)[1 + R \cdot e^{-ik2\ell}(\frac{1-e^{-iNk2d}}{1-e^{-ik2d}}) + higher \ \ order \ \ terms \ \ in \ \ R] \qquad (1)$$

where $k = \omega/c$ and N = 25. R is reflection coefficient of the incoming plane wave by a single slit. Note that $E_{ref}(\omega)$ in Eq. (1) provides a broad spectral background originated from the single-cycle nature of the source field, whereas the $R \cdot e^{-ik2\ell}(\dfrac{1-e^{-iNk2d}}{1-e^{-ik2d}})$ term supplies the multiple-resonance features spaced by a frequency interval of $\approx c/2d$.
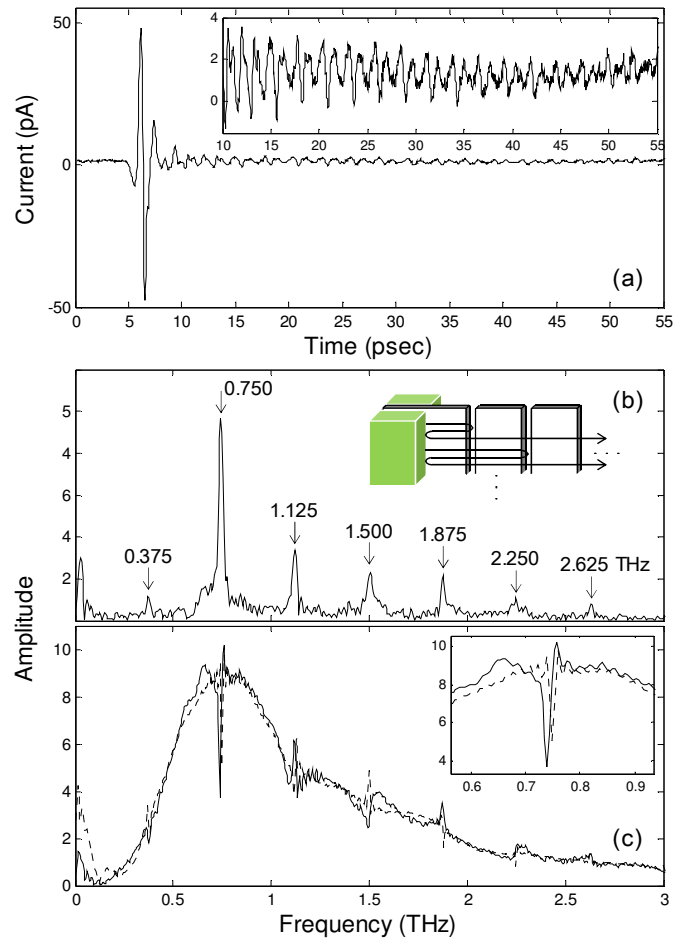
Fig. 2. (a) TSP pulse propagates on 1D array of slits. The inset shows the expanded data from 10 to 55psec. (b) Spectrum amplitude of reflection corresponding to the 10 to 55psec data. (c) Solid line renders the spectrum amplitude obtained using the whole measurement and the dashed line indicates the theoretical calculation. The inset shows the spectrum expanded at the resonance near 0.75THz.

   The interference of these two contributions results in the multiple Bragg resonance-like features shown in Fig. 2(c) that are composed of a maximum and a nearby minimum, very similar to Fano-like features [18]. Up to 55psec time domain data are used to calculate the spectrum. The background spectrum noisy is from unknown reflected pulses from the THz system especially around 1.2THz frequency range. It is remarkable the good agreement between the experimental data and the theoretical fitting using Eq. (1), shown in dashed line in Fig. 2(c). As R is very small, we neglect the higher order terms in Eq. (1), which describe the reflection by two or more slits. The calculated THz spectrum merits further comments. Through the fitting procedure, ℓ and R can be estimated to be 506μm and 0.017 ± 0.002, respectively. Note the good agreement between the measured ℓ (480μm) and the fitted result. We expect the reflection coefficient is not linear relation to the slit width. The relationship between slit width and reflection coefficient will research in future.
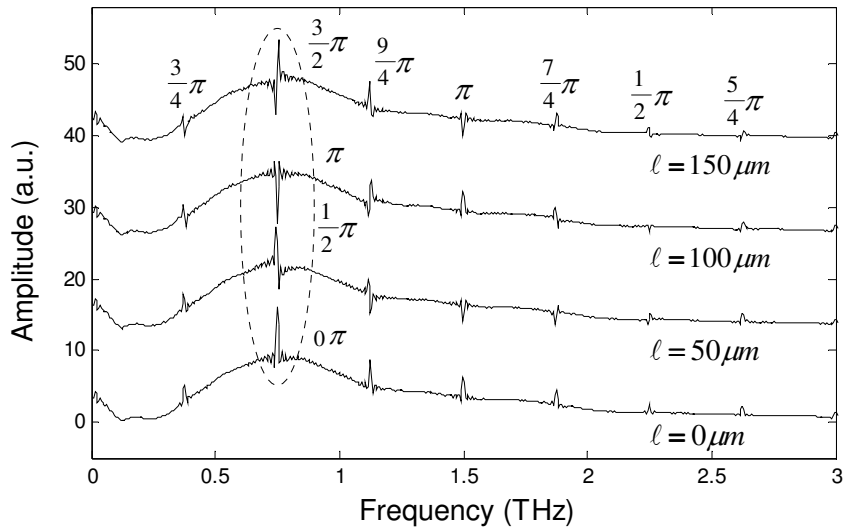
Fig. 3. Theoretical calculation with different length ℓ for a 400μm slit period.

The distance between the block and the first slit governs the overall sign of the multiple-path interference term in Eq. (1) through the exponential $e^{-ik2\ell}$. In order to show the role played by this parameter, we display in Fig. 3 the field amplitude obtained from Eq. (1) for R = 0.017 with different ℓ. The measured THz spectrum without the slits in the Al sheet is used for $E_{ref}(\omega)$. The numerator (e^{-iNk2d}) of Eq. (1) corresponds to small oscillation near the resonance. Therefore the background spectral noise shows up in the spectrum. The phase of the resonances depends on the resonant wavelength and ℓ. It is important to note that when ℓ is set to 0, all the resonances have the same sign (constructive interference as shown in bottom panel of Fig. 3).
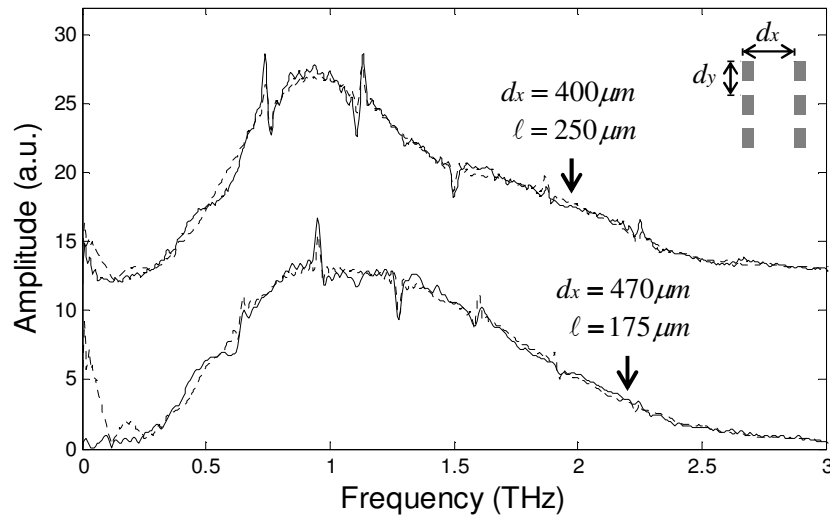

Fig. 4. Comparison of spectral resonances for different ℓ and d in rectangular hole arrays. Solid and dashed lines indicate experimental and theoretical results, respectively.

As we increase the length by 50μm intervals, Fano-like features indeed appear. At 0.75THz ($\lambda = 400\ \mu m$), indicated by a dashed circle in the figure, each increment of ℓ in 50μm leads to a resonance phase shift of $\pi/2$. When ℓ is equal to 150μm (top of Fig. 3), the phase of each resonance relative to the background depends on the frequency, and therefore, each resonance displays distinctive features. The broad background band is needed to display not only the constructive interference but also the distinctive interference.

We now discuss similar spectral features in THz waves propagating on rectangular hole arrays. When TSPs travel along a periodic arrangement of rectangular holes, the Bragg-reflection induced Fano-type spectral features are also observed as shown in Fig. 4. The holes are 80μm-width and 250μm-length, and the thickness of the sheet is 50μm. The upper panel shows the spectrum for a hole array whose period along the direction of propagation is $d_x = 400$μm and along the transversal direction $d_y = 330$μm. The lower spectrum corresponds to another sample with $d_x = 470$μm and $d_y = 400$μm. The lengths ℓ of the upper and the lower spectra are 250μm and 175μm, respectively. The dashed lines indicate calculated spectra showing good agreement with experiments. As a result of the fitting of our experimental data, we find that the reflection coefficient, R, of a single aperture (for both slits and rectangular holes) is also equal to 0.017 ± 0.002.

4. Theoretical calculations of the reflection coefficient
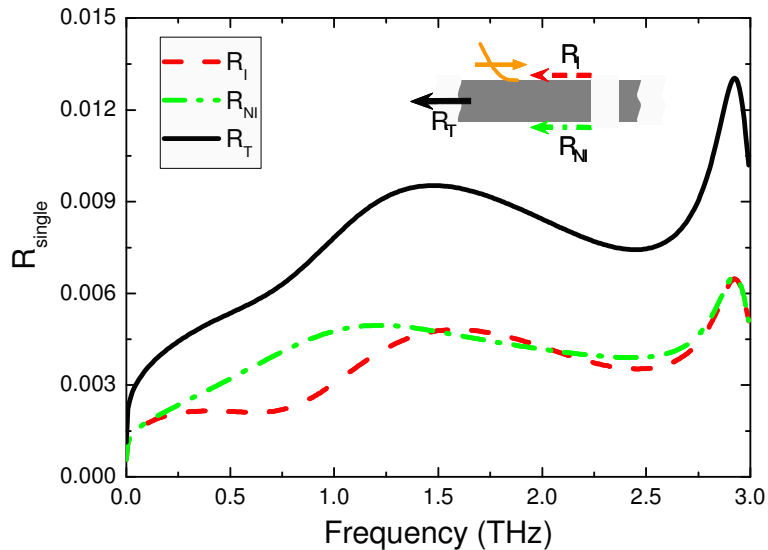

Fig. 5. Modulus of the reflection coefficients calculated with the modal expansion technique. R_I and R_{NI} denote the reflection coefficients for the illuminated and nonilluminated faces of the aluminum sheet, respectively. R_T is defined as the sum of the modulus of R_I and R_{NI}.

In order to check the value of R obtained from the fitting of our measurements to Eq. (1), we have carried out modal expansion calculations [19] of the scattering of THz SSPs by a single slit with the same geometry as considered in the experiments. The dielectric properties of the aluminum sheet are modeled through the surface impedance boundary conditions [20], which are an excellent approximation at THz frequencies. Two distinct coefficients are calculated, R_I and R_{NI} (see input Fig. 5), which describe the reflection of the SPPs at the illuminated, and non-illuminated side of the sheet, respectively. Figure 5 renders the modulus of these two reflection coefficients as a function of frequency within the spectral range

considered in the experiments. We have introduced another magnitude, R_T, which is defined as the sum of the modulus of the previous coefficients. R_T can be compared with the experimental value for R, as radiation coming from both sides of the film contributes to the signal measured in the far-field.

Note that the reflection coefficient in Fig. 5 shows a strong peaked feature at 2.8 THz. It is associated to the formation of Fabry-Perot like resonances inside the slit and along its depth. To a first approximation, the lowest resonant frequency is given by $f = c/2h = 3.0\,\text{THz}$, which is in good agreement with the spectral location of the maximum obtained through modal expansion calculations.

It is also remarkable the reasonable agreement between the measured frequency independent reflection coefficient and the theoretical spectrum shown in Fig. 5. The small discrepancy between the two magnitudes can be due to the approximations performed in Eq. (1), which does not take into account aspects such as higher order reflection waves, the coupling of through the slits, or the scattering out of plane of the TSP at the PPWG blocks.

We finally note that the sample parameters reported here are not conducive to observe strong features of designer surface plasmons. Due to the fact that the metal films considered in this experimental study are extremely thin, the flat part of the dispersion relation of the designer surface plasmons appears at very high frequencies and, therefore, the propagation characteristics of the TSPs are dominated by diffraction effects. Nevertheless our experimental and theoretical study provides the solid existence of Bragg reflections which will, with further analyses varying the geometrical parameters, lead us to observe more striking features in the future.

5. Conclusions

In conclusion, the propagation properties for TSP with slit and rectangular hole arrays have been studied in the THz regime. The spectral features result from the Bragg reflected multiple waves interfering with directly transmitted waves. The resulting spectra can in turn be used to deduce reflection coefficient associated with a single aperture. A theoretical model has been developed to describe the Bragg-reflection processes, which is in good agreement with the experimental results.

Acknowledgments